# Wideband Single-Pixel THz Imager in 28nm CMOS

S.L. van Berkel*, E.S. Malotaux†, M. Spirito†, D. Cavallo*, A. Neto* and N. Llombart*
*Terahertz Sensing Group, Department of Microelectronics, Delft University of Technology, Delft, The Netherlands
†Electronics Research Laboratory, Department of Microelectronics, Delft University of Technology, Delft, The Netherlands

***Abstract*—In this contribution, the simulated performance of a single pixel radiometer operating from 200 GHz to 600 GHz and integrated in 28nm CMOS technology is presented. With a simulated average system efficiency of 44% and Noise Equivalent Power (NEP) of 0.65 pW/$\sqrt{\text{Hz}}$ over the full operational bandwidth, the radiometer offers sub-Kelvin temperature sensitivity with real-time refresh rates, enabling low-cost imaging application in the sub-millimeter wave region of the EM-spectrum.**

## I. Introduction

THz imaging is promising for several types of applications such as security screening and remote sensing. State-of-the-art THz imagers are relying on the use of THz-sources [1] or cooling of the detectors [2] to obtain an image. Instead, passive (i.e. radiometric) and uncooled THz imagers are desired to enable low-cost imaging applications. In [3] it is shown that real-time THz radiometry, with sub-Kelvin temperature sensitivity, can be achieved when exploiting a large portion of the THz regime. The temperature sensitivity, $\Delta T$, of such system can be expressed as $\Delta T = \text{NEP}/(2k_B\Delta f_{RF}^{eff}\sqrt{\tau})$, where NEP is the detector noise equivalent power, $k_B$ the Boltzmann constant, $\tau$ the post detection integration time and $\Delta f_{RF}^{eff} = \bar{\eta}_{sys}\Delta f_{RF}$ is the effective bandwidth, defined as the average system efficiency times the absolute bandwidth. A single-pixel radiometer, operating between 200 GHz and 600 GHz and integrated in a 28nm CMOS technology, is designed to demonstrate real-time THz imaging with sub-Kelvin temperature sensitivity.

## II. Design

In order to achieve high imaging speeds with a good temperature sensitivity, both NEP and effective bandwidth should be optimized. To enable low-cost imaging applications, the antenna should suitable for CMOS integration (and therefore planar) and still operating efficiently over a broad portion of the THz spectrum. Novel integrated wideband antenna concepts that can be exploited in this kind of scenario are leaky-wave slot antennas [4]. These antennas have an airgap between the antenna and dense dielectric lens in order to illuminate the silicon dielectric lens more efficiently [5]. In the 28nm CMOS stratification, available for the prototype, there is not such an airgap. However, the antenna is printed in the top metal layer, which is separated by approximately 5 $\mu m$ of $SiO_2$ from the low-resistive silicon. This thin $SiO_2$ introduces a slight enhanced leaky-wave behavior which enables a double bow-tie slot antenna [6] to operate efficiently with clean and stable patterns over a bandwidth from 200 GHz to 600 GHz. In the antenna optimization, one should take the finiteness of the GND-plane into account. The antenna is optimized in transmission in CST Microwave Studio. The schematic side-view of the CMOS stratification and a micrograph of the fabricated double bow-tie slot (with dimensions (in $\mu m$)) are shown in Fig. 1. A quasi-optical system, containing dielectric lenses, is required to focus the radiation from a small spot in an image plane to the double bow-tie slot antenna and is also illustrated in Fig. 1. The low-resistive silicon of the chip, thinned down to 200 $\mu m$ to reduce ohmic dissipation, is glued to a silicon elliptical lens with matching layer. Incident radiation coming from an image plane that is designed to be 20 cm from the radiometer, is focused via a hyperbolic lens and two flat mirrors to the elliptical lens.

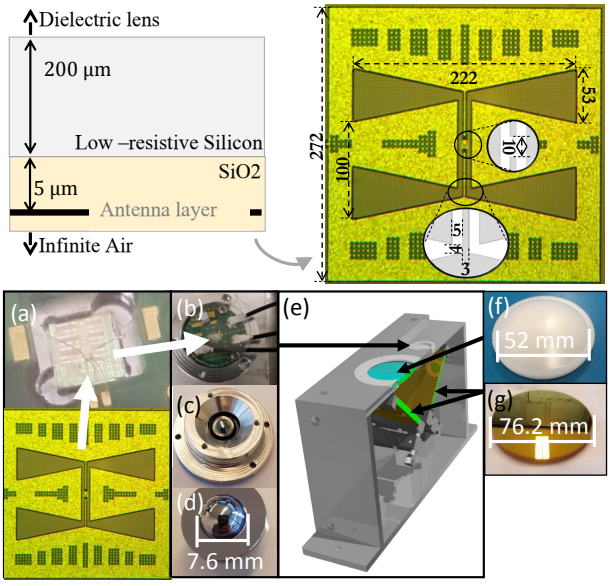


Fig. 1. The dimensions are shown of the double-bow tie slot antenna that is printed in the top metal layer of the 28nm CMOS stratification. The detector read-out pads on the CMOS chip are bondwired to a PCB (a,b) after the chip is glued to an elliptical lens that is fixed in a metallic holder (c,d). The elliptical lens is fixed in a quasi-optical system (e) and coupled to a hyperbolic mirror (f) via two flat mirrors (g) in order to create an image plane 20 cm from the radiometer.

The second important parameter that can be optimized, is the noise that is introduced by the detector. THz detectors suitable for CMOS integration that are commonly used are Schottky-diodes and MOSFETS. However, these devices are prone to high flicker noise (i.e. 1/f noise) contributions [7], [8]. A low 1/f corner frequency is desirable in order to be able to modulate the input signal beyond the 1/f corner frequency,

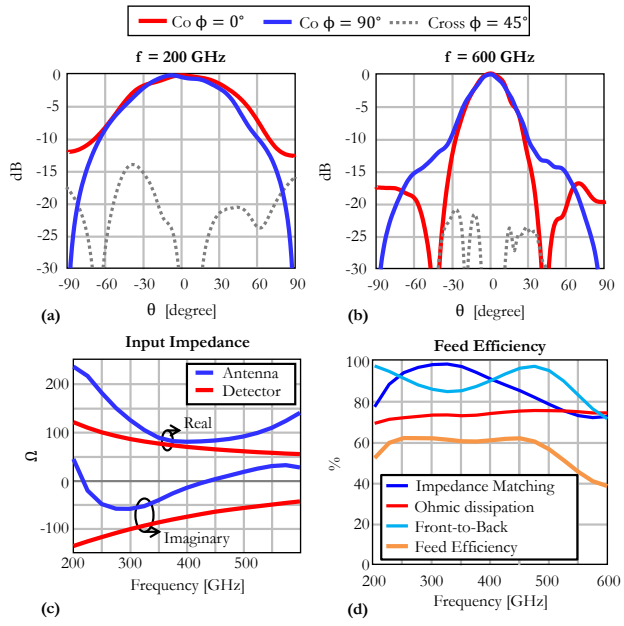


Fig. 2. Normalized radiation patterns inside infinite silicon at (a) 200 GHz and (b) 600 GHz. The input impedances of the detector and antenna are shown in (c) and the feed efficiency (omitting losses in the quasi-optical components) is shown in (d).

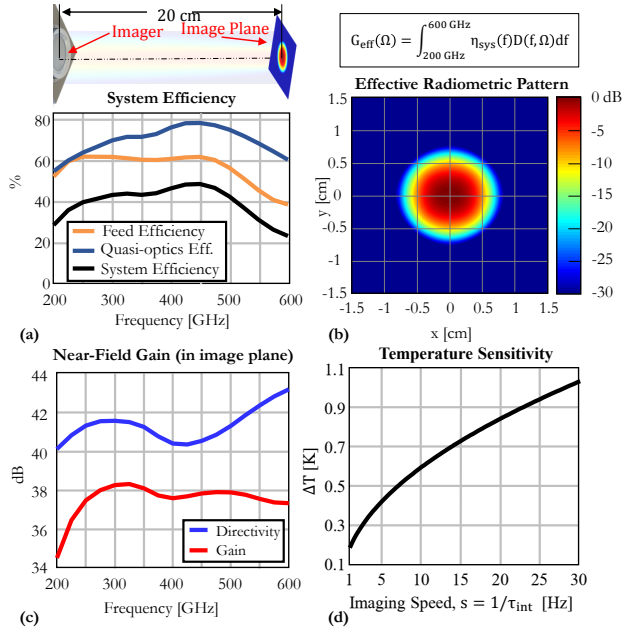


Fig. 3. The summarized performance of the complete system. In (a) the system efficiency is shown, introducing the efficiency of all quasi-optical components. In (b) the effective radiometric pattern and its definition are shown. In (c) the directivity and gain in the image plane are shown. In (d) the temperature sensitivity of the radiometer is shown as function of imaging speed.

into the white-noise region. In this design we aim to use a pn-junction diode because such diodes are able to provide good voltage responsivity over the full operational bandwidth while simultaneously offering a low 1/f corner frequency [9]. Pn-junction devices are readily available and characterized in the available CMOS technology and is optimized in both noise and impedance matching with the antenna.

## III. Results

The antenna patterns, simulated in CST and radiating inside infinite silicon, at 200 GHz and 600 GHz are shown in Fig. 2(a) and (b) respectively. The input impedance, for both antenna and detector, are shown in Fig. 2(c). The feed efficiency of the antenna, i.e. without any quasi-optical components, is shown in (d) and contains the impedance matching, front-to-back ratio and ohmic dissipation in the silicon and metals of the technology. The system efficiency of the radiometer is shown in Fig. 3(a) and includes all losses in the quasi-optical system.

In radiometry, since the radiometer integrates power incoherently over the full bandwidth and no spectral information can be resolved in the output signal, a suitable way to evaluate the imaging performance of the quasi-optical system is by calculating it's effective radiometric pattern which is defined as the spectral integration of the near-field gain (shown in (c)) in the image plane [3]. The effective radiometric pattern and its definition are shown in Fig. 3(b) and features a -3 dB spot-size of approximately 1 cm in diameter.

The average system efficiency over the full operational frequency band is 43.7 % and translates to an effective bandwidth of $\Delta f_{RF}^{eff} = \bar{\eta}_{sys} \Delta f_{RF} = 175$ GHz. The detector, optimized in noise and antenna-detector matching, has an average NEP of $NEP = 0.65$ pW/$\sqrt{\text{Hz}}$. The temperature sensitivity, using the effective bandwidth and NEP, is shown in Fig. 3(d) as function of imaging speed $s = 1/\tau_{int}$. It can be seen that sub-Kelvin imaging capabilities can be achieved at real-time refresh rates, enabling low-cost imaging application in the sub-millimeter wave region of the electromagnetic spectrum.

## Acknowledgement

This research is supported by the Dutch Technology Foundation STW (TiCAM, 13325) and ERC starting grant LAA-THz-CC (639749).

## References

[1] R. A. Hadi, et.al., "A 1 k-pixel video camera for 0.7-1.1 Terahertz imaging applications in 65-nm CMOS," *IEEE JSSC*, vol. 47, no. 12, pp. 2999–3012, Dec. 2012.
[2] A. Timofeev, et.al., "Optical and electrical characterization of a large kinetic inductance bolometer focal plane array," *IEEE TTST*, 2017.
[3] S. van Berkel, et.al., "THz imaging using uncooled wideband direct detection focal plane arrays," *IEEE TTST*, 2017.
[4] O. Yurduseven, et.al., "A dual-polarized leaky lens antenna for wideband focal plane arrays," *IEEE TAP*, 2016.
[5] A. Neto, "UWB, non dispersive radiation from the planarly fed leaky lens antenna - part 1: Theory and design," *IEEE TAP*, 2010.
[6] A. J. Alazemi, et.al., "Double bow-tie slot antennas for wideband millimeter-wave and Terahertz applications," *IEEE TTST*, 2016.
[7] R. Han, et.al., "Active Terahertz imaging using Schottky diodes in CMOS: Array and 860-GHz pixel," *IEEE JSSC*, 2013.
[8] D. Y. Kim, et.al., "Design and demonstration of 820-GHz array using diode-connected NMOS transistors in 130-nm CMOS for active imaging," *IEEE TTST*, 2016.
[9] Z. Ahmad and O. K. K, "THz detection using $p^+$/n-well diodes fabricated in 45-nm CMOS," *IEEE EDL*, 2016.